ACS APPLIED MATERIALS & INTERFACES

RESEARCH ARTICLE

www.acsami.org

Enhanced Electrical Conductivity in Polystyrene Nanocomposites at Ultra-Low Graphene Content

Xian-Yong Qi,[†] Dong Yan,[†] Zhiguo Jiang,[†] Ya-Kun Cao,[†] Zhong-Zhen Yu,[*,†] Fazel Yavari,[‡] and Nikhil Koratkar[*,‡]

[†]State Key Laboratory of Organic−Inorganic Composites, Department of Polymer Engineering, College of Materials Science and Engineering, Beijing University of Chemical Technology, Beijing 100029, China

[‡]Department of Mechanical, Aerospace and Nuclear Engineering, Rensselaer Polytechnic Institute, Troy, New York 12180, United States

Supporting Information

ABSTRACT: We compared the electrical conductivity of multiwalled-carbon-nanotube/polystyrene and graphene/polystyrene composites. The conductivity of polystyrene increases from ∼6.7×10^{-14} to ∼3.49 S/m, with an increase in graphene content from ∼0.11 to ∼1.1 vol %. This is ∼2−4 orders of magnitude higher than for multiwalled-carbon-nanotube/polystyrene composites. Furthermore, we show that the conductivity of the graphene/polystyrene system can be significantly enhanced by incorporation of polylactic acid. The volume-exclusion principle forces graphene into the polystyrene-rich regions (selective localization) and generates ∼4.5-fold decrease in its percolation threshold from ∼0.33 to ∼0.075 vol %.

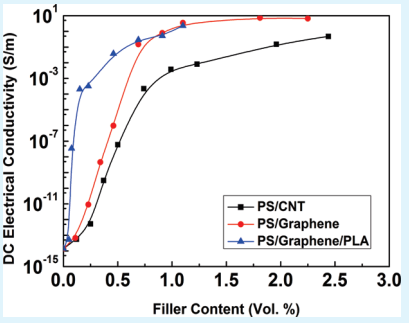

KEYWORDS: graphene, polystyrene, polylactic acid, electrical conductivity, percolation threshold, selective localization, volume exclusion

Much attention has been paid to graphene due to its two-dimensional structure, large specific surface area, ease of manufacture (top down synthesis by exfoliation of graphite), and superior properties.[1,2] In particular, the utilization of graphene as an electrically conductive additive in nanocomposites shows significant potential for practical applications. The theoretical study of Xie et al.[3] predicts that graphene is more effective for conductivity enhancement than other competing nanofillers such as carbon nanotubes because of its large specific surface area. However, there have been contradictory reports in the literature with some studies[4] reporting that graphene is less effective than carbon nanotubes in forming conductive networks. Therefore, the purpose of the present work is to compare the efficiency of graphene with that of carbon nanotubes in improving electrical conductivity in polymer composites. The specific polymer system chosen for this study is polystyrene (PS). Additionally, the volume-exclusion (or selective localization) principle[5−8] is employed to further decrease the percolation threshold of the electrically conductive graphene/PS composites. Although selective localization of carbon black[5] and carbon nanotubes[6−8] has been shown to reduce percolation threshold in polymers, to the best of our knowledge, there is no prior report on the selective localization of graphene in polymer nanocomposites. We demonstrate in this work that selective localization of graphene in PS due to incorporation of polylactic acid (PLA) into the PS/graphene composite drastically reduces the percolation threshold value by a factor of ∼4.5 from ∼0.33 to ∼0.075 vol %.

The graphene platelets used in this study were obtained by the one-step thermal exfoliation and reduction of graphite oxide (see the Supporting Information). In this method, graphite oxide is subjected to a thermal shock (rapid rate of heating ∼2000 °C/min) that exfoliates and reduces the graphite oxide into graphene platelets.[9−12] Transmission electron microscopy and X-ray diffraction characterization of the graphene produced in this manner is provided in the Supporting Information. The multiwalled carbon nanotubes (CNT) used in the present work (purity >95% and outer diameters of ∼20−30 nm) were procured from Chengdu Organic Chemicals Co. Ltd. (China). PLA (2002D) was obtained from NatureWorks (United States) with an average molecular weight of about 160 000−220 000 g/mol. PS with an average molecular weight of 158 000 g/mol was purchased from BASF-YPC (China). Graphene/PS and CNT/PS nanocomposites were prepared by solution mixing followed by compression molding. Briefly ∼10 g of PS was dissolved in ∼60 mL dimethyl formamide (DMF) at ∼45 °C. The desired amounts of CNT or graphene were first dispersed in DMF (∼0.1 g nanofiller per 100 mL DMF) by ultrasonic exfoliation for ∼1.5 h using a KQ-250DB sonicator at 250 W. Then, the suspension of CNT or graphene was added into the PS solution. After the mixture was mechanically stirred for ∼2 h, it was dropped into a large volume of vigorously stirred methanol to coagulate the PS nanocomposites, which was then filtered and dried in a circulating oven at ∼80 °C for ∼16 h followed by drying in a vacuum oven at ∼120 °C for ∼12 h. Finally, the dried nanocomposites

Received: May 17, 2011
Accepted: July 11, 2011
Published: July 11, 2011

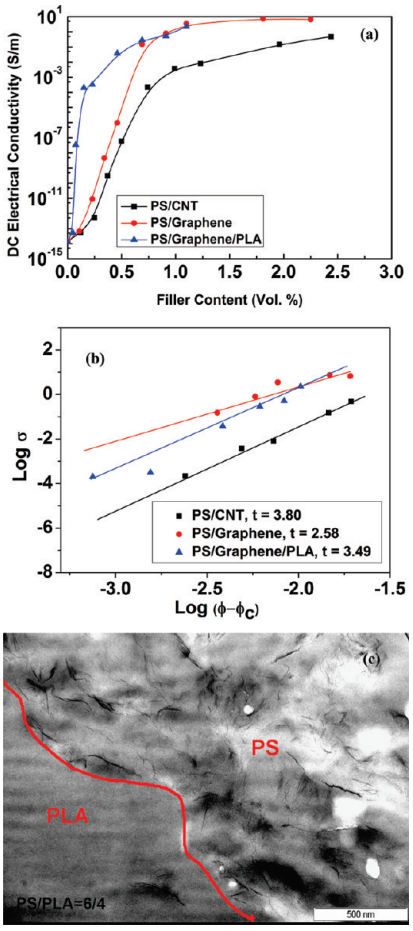

Figure 1. (a) Electrical conductivity versus filler content for neat PS and its nanocomposites. (b) Double-logarithmic plot of electrical conductivity versus $(\varphi - \varphi_c)$, where φ is the filler volume fraction and φ_c is the percolation threshold. (c) TEM image of PS/PLA (6/4) composite with ~0.46 vol % (~1.0 wt %) graphene additives. 6/4 indicates ~60% PS and ~40% PLA. The selective localization of graphene in the PS region is evident from the image.

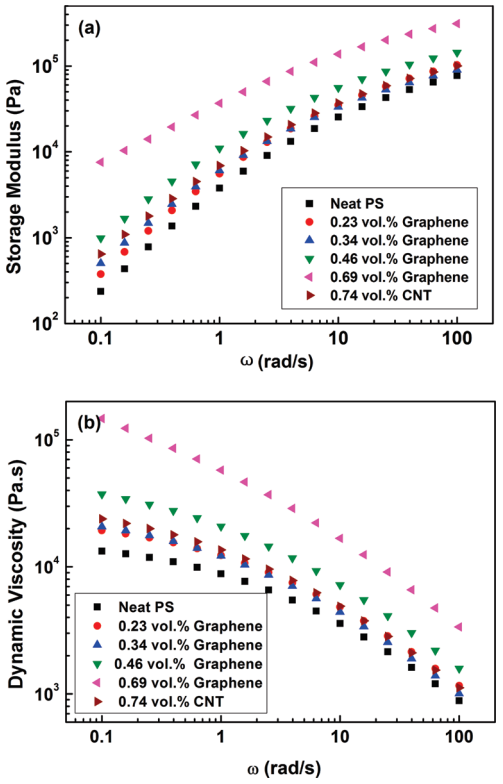

Figure 2. (a) Storage modulus and (b) dynamic viscosity versus frequency for neat PS and PS nanocomposites measured at ~200 °C. The graphene composites show markedly higher storage moduli and dynamic viscosity as compared to the pristine PS and CNT/PS nanocomposites.

were hot-pressed into ~1-mm thick plates using a Beijing Kangsente KT-0906 vacuum hot press at ~200 °C and ~10 MPa. The same procedure was also used to prepare PS/PLA/graphene nanocomposites.

The volume conductivities of PS and its nanocomposites with lower conductivity than 10^{-6} S/m were measured by a ZC-90G resistivity meter from Shanghai Taiou Electronics (China). The volume conductivities of PS nanocomposites with conductivity higher than 1×10^{-6} S/m were measured by Keithley 4200-SCS (USA) using a standard four-probe method. Figure 1a shows the electrical conductivities of the PS nanocomposites. It is clear that graphene is more effective in improving the electrical conductivity of PS than CNT, evidenced by higher electrical conductivity and smaller percolation threshold. The electrical conductivities of the PS/graphene nanocomposites show a rapid increase from ~6.7×10^{-14} to ~0.15 S/m, when the graphene content is increased from ~0.11 to ~0.69 vol %. The addition of ~1.1 vol % graphene endows PS with an electrical conductivity as high as ~3.49 S/m. However, for the CNT/PS nanocomposite with the same content of CNT (~0.69 vol %), its conductivity is only ~3×10^{-5} S/m, which is nearly 4 orders of magnitude lower in comparison to the graphene/PS nanocomposite. As demonstrated by Xie et al.,[3] compared to one-dimensional CNT, 2-dimensional graphene nanosheets can form a conducting network at a lower content due to the latter's higher specific surface area, which is consistent with our results.

The power-law equation[13] is widely used to study the relationship between filler content and electrical conductivity

$$\sigma = \sigma_0(\varphi - \varphi_c)^t$$

where σ is the electrical conductivity of composites, σ_0 is a constant that is typically assigned to the plateau conductivity of fully loaded composites, φ is the filler volume fraction, φ_c is the percolation threshold, and the exponent (t) is used to interpret the mechanism of network formation. For the double-logarithmic plot (Figure 1b) of the electrical conductivity versus $(\varphi - \varphi_c)$, where φ_c values are 0.50 and 0.33 vol %, the values of t are 3.80 and 2.58 for PS/CNT and PS/graphene nanocomposites, respectively. Several works have studied cluster statistics and percolation characteristics in 1D and 2D lattice systems.[14−17] These studies indicate that aspect ratio plays an important role in determining the "t" value. For instance the theoretical and computational study by Foygel et al.[16] predicts that t decreases from ~2.2 to ~1.2 with an increase in the aspect ratio from ~1 to ~1000. In our work, the t value for the CNT is much higher than for graphene fillers which indicates an higher "effective aspect ratio" for the graphene as compared to the CNT in the PS matrix.

Dynamic frequency sweep tests were also performed to explore network formation in the nanocomposites by studying the variation of the storage modulus (G′) with frequency

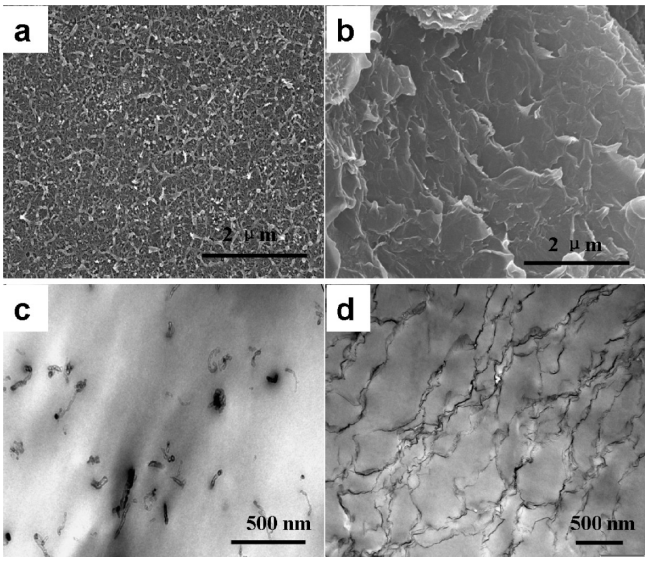

Figure 3. SEM images of freeze-fractured surfaces of PS nanocomposites with (a) 0.74 vol % (~1.5 wt.%) CNT and (b) 0.69 vol % (~1.5 wt %) graphene. TEM images of (c) PS/1.5 wt % CNT and (d) PS/1.5 wt % graphene nanocomposites.

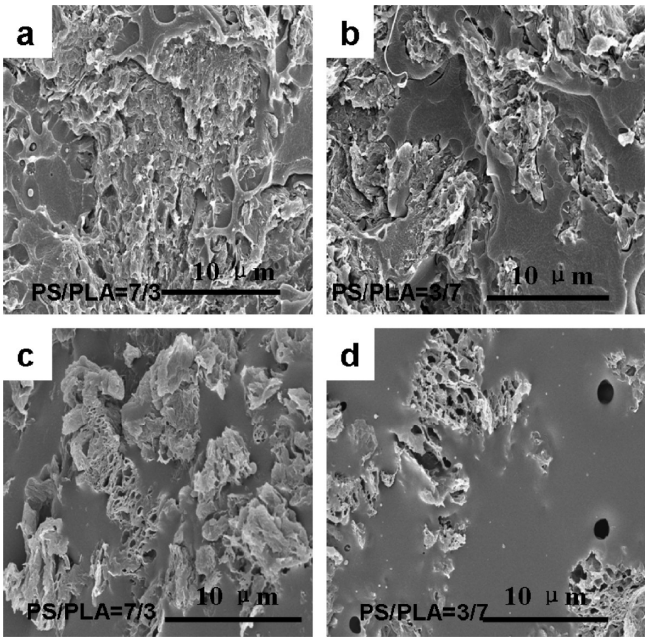

Figure 4. SEM images of freeze-fractured surfaces of (a, c) PS/PLA (7/3) and (b, d) PS/PLA (3/7) nanocomposites filled with 0.46 vol % (~1.0 wt %) graphene (a, b) before and (c, d) after etching with acetone. Acetone is a solvent of PS. 7/3 indicates 70% PS and 30% PLA, whereas 3/7 indicates 30% PS and 70% PLA.

(Figure 2a). At low frequency (~0.1 rad/s), the storage modulus of PS rapidly increases from 230 to 1000 Pa, after adding ~0.46 vol % graphene. When the content of graphene is ~0.69 vol %, the storage modulus reaches ~7800 Pa. By contrast, CNT do not significantly enhance the storage modulus of the composites (for instance at ~0.74 vol % CNT, G′ is only 640 Pa). These results suggest that compared to CNT, graphene can form a pseudosolid-like network more easily, possibly due to its greater interfacial contact area. Complex viscosity (η^*) of the graphene/PS and CNT/PS composites is shown in Figure 2b. While neat PS exhibits a plateau in complex viscosity (~13 000 Pa s), the curves of graphene/PS nanocomposites exhibit viscosity plateaus, ranging from ~20 160 Pa.s at ~0.34 vol % to ~144 000 Pa s at ~0.69 vol %. Importantly, nanocomposites filled with graphene exhibit significantly higher viscosity than CNT over the full range of frequencies tested. This indicates that the cross-link density of the graphene/PS network is higher than that of the CNT/PS network which is consistent with the higher electrical conductivity of the graphene/PS nanocomposites shown in Figure 1a.

Further, we find that incorporation of PLA greatly improves the conductivity and reduces the percolation threshold of PS/graphene nanocomposites (Figure 1a). PS/PLA composites with ~60% PS and ~40% PLA was used in the testing. With 0.15 vol % of graphene, the conductivity of the ternary graphene/PS/PLA nanocomposite reaches ~2.05×10^{-4} S/m. To achieve the same value in the PS/graphene binary nanocomposite, ~0.57 vol % of graphene is required. The percolation threshold of the graphene/PS/PLA ternary nanocomposites is ~0.075 vol %, which is ~4.5-fold lower than the PS/graphene binary nanocomposite. This result can be explained by selective localization of graphene in the PS/PLA components. Transmission electron microscopy (TEM) image of the nanocomposite (Figure 1c) indicates that the graphene nanosheets are selectively located in PS matrix, rather than in PLA phase. This selective localization of the graphene sheets results in a networked structure at relatively lower graphene content, which serves to significantly reduce the percolation threshold and increase the electrical conductivity of the nanocomposite.

We also investigated the morphologies of the nanocomposties using scanning electron microscopy (SEM) analysis. The SEM image (Figure 3b) reveals that overall the graphene does not agglomerate into dense regions. This could be related to favorable $\pi-\pi$ interactions between the graphene sheets and polystyrene. Figure 3a indicates the corresponding SEM micrograph of the CNT/PS binary nanocomposite. Some agglomerations were found, and compared to graphene the CNT do not disperse as uniformly in the PS matrix. This is also confirmed by the transmission electron microscopy (TEM) micrograph shown in Figure 3c. Some dark spots were found in the picture, which represent CNT agglomerations. By contrast, the TEM micrograph of graphene is much different, as indicated in Figure 3d. Extensive TEM showed no evidence of multilayer stacks. Graphene nanosheets were homogeneously dispersed in the PS matrix, and a continuous network structure was formed. This explains why the electrical conductivity of the graphene/PS nanocomposite is markedly superior to the CNT/PS nanocomposite.

Images a and b in Figure 4 show SEM micrographs of the fractured surfaces of graphene/PS/PLA ternary nanocomposites for different PS/PLA ratios. In Figure 4a, most part of the image is rough, which indicates the presence of graphene. Moreover the PS matrix is continuous phase, owing to its higher content (70 wt %). As a result, we conclude that the graphene is uniformly dipsersed in the PS matrix. When the content of PLA reaches ~70 wt.% (shown in Figure 4b), there are primary surfaces with smooth topology in the image. This smooth texture indicates that graphene sheets are not present in the PLA region. To further study this the nanocomposites were etched by acetone, a solvent of PS rather than PLA. After etching for ~5 min, most of the PS was removed. The SEM microphotographs of etched graphene/PS/PLA nanocomposites are provided in images c and d in Figure 4. A comparison of Figure 4a with Figure 4c shows that the

graphene is indeed located in the PS matrix. Comparing Figure 4c with Figure 4d, we find that the coarse surface is greater in Figure 4c. This demonstrates that graphene selectively distributes into the PS matrix. There are three reasons for this: (1) the graphene was compounded with PS, followed by the addition of PLA solution into the graphene/PS blend. Naturally, graphene would combine with the PS first. (2) The viscosity of PLA is much higher than PS, resulting in its poor liquidity. Consequently, during processing, graphene intercalated into the PS matrix, and PLA was isolated in the matrix, as shown in Figure 4c. (3) The polarity of graphene is similar with PS, but not well matched with that of PLA. After thermal reduction, most of the polar functional groups are expelled from graphene,[10−12] which makes the graphene less polar. But PLA is polar and crystalline, which are unfavorable for bonding with the graphene. All of these factors contribute to selective localization of the graphene in the PS regions, which promotes the formation of electrically conductive networks at exceedingly low graphene content.

■ ASSOCIATED CONTENT

Supporting Information. Protocols used to synthesize graphene, X-ray diffraction, and transmission electron microscopy images of the as-produced graphene platelets and X-ray diffraction analysis of the nanocomposites. This material is available free of charge via the Internet at http://pubs.acs.org/.

■ AUTHOR INFORMATION

Corresponding Author
*E-mail: yuzz@mail.buct.edu.cn (Z.Y.); koratn@rpi.edu (N.K).

■ ACKNOWLEDGMENT

Financial support from the National Natural Science Foundation of China (50873006, 51073012) and the Program for New Century Excellent Talents in Universities, Ministry of Education of China (NCET-08-0711) are gratefully acknowledged. N.K. acknowledges funding support from the U.S. Office of Naval Research (Award N000140910928) and the USA National Science Foundation (Award 0900188).

■ REFERENCES

(1) Geim, A. K. *Science* **2009**, *324*, 1530–1534.
(2) Rao, C. N. R.; Sood, A. K.; Subrahmanyam, K. S.; Govindaraj, A. *Angew. Chem., Int. Ed.* **2009**, *48*, 7752–7777.
(3) Xie, S.; Liu, Y.; Li, J. Y. *Appl. Phys. Lett.* **2008**, *92*, 243121.
(4) Du, J. H.; Zhao, L.; Zeng, Y.; Zhang, L. L.; Li, F.; Liu, P. F. *Carbon* **2011**, *49*, 1094–1100.
(5) Gubbels, F.; Vanlathem, S. B. E.; Jerome, R.; Deltour, R.; Brouers, F.; Teyssie, P. *Macromolecules* **1995**, *28*, 1559–1566.
(6) Potschke, P.; Bhattacharyya, A. R.; Janke, A. *Polymer* **2003**, *44*, 8061–8069.
(7) Meincke, O; Kaempfer, D.; Weickmann, H.; Friedrich, C.; Vathauer, M.; Warth, H. *Polymer* **2004**, *45*, 739–748.
(8) Dasari, A.; Yu, Z.-Z.; Mai, Y. W. *Polymer* **2009**, *50*, 4112–4121.
(9) Zhang, H. B.; Wang, J. W.; Yan, Q.; Zheng, W. G.; Chen, C.; Yu, Z.-Z. *J. Mater. Chem.* **2011**, *21*, 5392–5397.
(10) Srivastava, I.; Mehta, R. J.; Yu, Z.-Z.; Schadler, L.; Koratkar, N. *Appl. Phys. Lett.* **2011**, *98*, 063102.
(11) Rafiee, J.; Rafiee, M. A.; Yu, Z.-Z.; Koratkar, N. *Adv. Mater.* **2010**, *22*, 2151–2154.
(12) Yavari, F.; Rafiee, M. A.; Rafiee, J.; Yu, Z.-Z.; Koratkar, N. *ACS Appl. Mater. Interfaces* **2010**, *2*, 2738–2743.
(13) Stauffer, D.; Aharony, A. *Introduction to Percolation Theory*; Taylor & Francis: London, 1992; pp 89−113.
(14) Deng, F.; Zheng, Q. S.; Wang, L. F.; Nan, C. W. *Appl. Phys. Lett.* **2007**, *90*, 021914.
(15) Yao, S. H.; Dang, Z. M.; Jiang, M. J.; Xu, H. P. *Appl. Phys. Lett.* **2007**, *91*, 212901.
(16) Foygel, M.; Morris, R. D.; Anez, D.; French, S.; Sobolev, V. L. *Phys. Rev. B* **2005**, *71*, 104201.
(17) Yoonessi, M.; Gaier, J. R. *ACS Nano* **2010**, *4*, 7211–7220.